Iğdır Üniversitesi Fen Bilimleri Enstitüsü Dergisi, 15(2), 634-649, 2025
Journal of the Institute of Science and Technology, 15(2), 634-649, 2025
ISSN: 2146-0574, eISSN: 2536-4618
Chemical Engineering **DOI: 10.21597/jist.1522708**
Research Article
Received: 26.07.2024 **Accepted: 24.10.2024**

To Cite: Uğur, M., Yartaşı, A. & Kocakerim, M. M. (2025). Kinetic Behavior of Ca^{2+} Ions During the Dissolution of Colemanite in Propionic Acid Solutions. *Journal of the Institute of Science and Technology*, 15(2), 634-649.

Kinetic Behavior of Ca^{2+} Ions During the Dissolution of Colemanite in Propionic Acid Solutions

Mücahit UĞUR[1*], Ahmet YARTAŞI[1], M. Muhtar KOCAKERİM[1]

Highlights:

- Investigation of Ca^{2+} dissolution kinetics of colemanite in solutions saturated with propionic acids.
- It has been determined that the speed expression of the process fits the Avrami model.
- A mathematical model was determined based on the influence of dissolution parameters.
- A new reactant capable of dissolving colemanite has been identified.

Keywords:

- Boron
- Colemanite
- Propionic acid
- Dissolution kinetics
- Activation energy

ABSTRACT:

The leading commercial boron reserves in Türkiye are colemanite, tincal, and ulexite. The Colemanite ore, a calcium borate mineral, has the richest composition in terms of boron trioxide (B_2O_3). Boric acid, with its high B_2O_3 content, is the basic raw material in the production of boron compounds in industry. The use of boron and boron derivatives is increasing in today's industry. The boron minerals to be used must be obtained in pure form. Dissolving colemanite in propionic acid prevents the formation of impurities and produces a commercially important by-product This study, conducted on the dissolution kinetics of colemanite in propionic acid solutions, shows that parameters reaction temperature, acid concentration, solid-liquid ratio, and particle size significantly affect the dissolution rate and that the dissolution efficiency can be increased by optimizing these parameters. These findings are compatible with other studies in the literature and provide important contributions to research on the dissolution kinetics of colemanite in different acid solutions. As a result, it has been observed that stirring speed has no effect in most of these studies on dissolution kinetics of colemanite in different acid solutions. It has been established that the dissolution rate typically rises with elevated temperatures, diminished particle size, and reduced solid-liquid ratio. These results, in which the dissolution process mostly depends on diffusion control and the activation energy is calculated, are consistent with the findings obtained in propionic acid solutions. The activation energy (E) was found to be 36.56 kj/mol.

---

[1] Mücahit UĞUR (**Orcid ID:** 0000-0002-3746-5683), Ahmet YARTAŞI (**Orcid ID:** 0000-0003-0469-4575), M. Muhtar KOCAKERİM (**Orcid ID:** 0000-0003-3276-6097), Cankiri Karatekin University, Faculty of Engineering, Department of Chemical Engineering, Cankiri, Türkiye

***Corresponding Author:** Mücahit UĞUR, e-mail: m.ugur@karatekin.edu.tr

This study was produced from Mücahit UĞUR's PhD thesis.

INTRODUCTION

Boron ore is one of the most commercially exploited ores globally, largely due to its superior properties. Boron and boron minerals have an increasing usage area and amount. Approximately 10% of the boron minerals produced are used directly as minerals and the remaining 90% are used to obtain boron products (Küçük et al., 2023). The different properties of boron and boron compounds when combined with various metal or nonmetal elements provide a wide range of uses in industry (Uğur, 2024a). Boron and boron products are used in ceramics, textiles, cosmetics, cleaning and whitening, high-quality steel, agriculture and catalyst (Küçük et al., 2023), heat-resistant polymers (Uğur et al., 2024), nuclear technology (Çalımlı et al., 2020), agriculture and fire retardant, energy storage, defense industry, waste storage (Uğur, 2024b), electronics, communication and automotive (Kavcı et al., 2014).

Approximately 73% of the world's 4.5 billion tons of boron compounds are located in Turkey (Çopur et al., 2022). These ores, the ones that have commercial importance in terms of quantity are colemanite, tincal, ulexite, and kernite (Guliyev et al., 2012; Tombal et al., 2016). Colemanite, used as raw material in the production of boric acid, is characterized by its calcium structure and monoclinic crystal structure. Boric acid is the most commonly utilized boron compound in industrial contexts (H_3BO_3). Boric acid is obtained through industrial processes involving the reaction of colemanite with sulfuric acid. (Kaya & Özer, 2024).

$$2CaO.3B_2O_3.5H_2O + 2H_2SO_4 + 6H_2O \rightarrow 6H_3BO_3 + 2CaSO_4.2H_2O \qquad (1)$$

Table 1. Literature Research on Dissolution Kinetics of Colemanite Ore with Different Leaching Solutions

Leaching Solution	Rate control model	Activation energy (E) kj/mol	Reference
Pyrite roasting gas, propionic acid	Avrami Model	38.66	(Uğur, 2024b)
Sodium bisulfate	Ash film is diffusion-controlled in two stages	3.4 and 6.1	(ŞİMŞEK & YEŞİLYURT, 2021)
Di ammonium hydrogen phosphate	First-order pseudo homogenous model	42.10	(Şimşek et al., 2018)
Potassium dihydrogen phosphate	Chemical reaction controlled	41.88	(Karagöz & Kuşlu, 2017)
Methanol	Second-order pseudo homogenous model	51.4	(Kizilca & Copur, 2015)
Oxalic acid	First- order pseudo homogenous model	27.88	(Bayca et al., 2014)
Ammonium carbonate	First-order pseudo homogenous model	59.03	(Künkül et al., 2012)
Ammonium hydrogen sulfate	Ash film diffusion controlled	32.66	(Guliyev et al., 2012)
Perchloric acid	Chemical reaction controlled	46.76	(Gür & Alkan, 2008)
Sulfuric acid	Ash film diffusion controlled	41.40	(Gür, 2007)
Sulfur dioxide gas	Avrami model	50.14	(Kurtbaş et al., 2006)
Citric acid	Ash film diffusion controlled	28.65	(Çavuş & Kuşlu, 2005)
Oxalic acid	Ash film diffusion controlled	39.71	(Alkan & Doğan, 2004)
Sulfur dioxide gas	Chemical reaction controlled	39.53	(Küçük et al., 2002)
Sulfuric acid	Surface chemical reaction	28.96	(Temur et al., 2000)
Phosphoric acid	Surface chemical reaction	53.9	(Alkan et al., 2000)

Due to the strong acidic properties of sulfuric acid, it dissolves gangue minerals and colemanite. Impurities such as Ca^{2+} and Mg^{2+} in colemanite and SO_4^{2-} resulting from sulfuric acid cause impurities in the product (Tombal et al., 2016; Tunç et al., 2007). This situation reduces the quality and efficiency of boric acid. Furthermore, as illustrated in Reaction (1), borogypsum, a by-product of the process, is stored in lakes that have been created artificially for this purpose, along with boric acid. Borogypsum forms the basis of soil and environmental pollution (Kum et al., 1994; Tunç et al., 2007). In addition, H_2SO_4 causes serious corrosive effects in factory and reactor systems (Karagöz & Kuşlu, 2017). To minimize these situations, it would be more appropriate to use weakly acidic solutions (Sert et al., 2012).

Due to the basic character of colemanite ore, the most suitable reagents to be used in dissolving colemanite are acids (Şimşek & Yeşilyurt, 2021). A substantial body of literature exists on the processes of colemanite ore in acidic gases and solutions. The activation energies and speed control models of the processes under investigation are summarised in Table 1.

This study investigated how Ca^{2+} passes into solution during colemanite dissolution in propionic acid, aiming to reduce impurities and identify a new reactant for boric acid production. When colemanite is dissolved in propionic acid, boric acid is produced and calcium propionate [$Ca(CH_3CH_2COO)_2$] is formed as a by-product. Calcium propionate, an industrially valuable compound, is utilized in the bakery, bread, and food industries for the preservation of baked goods from microbial contamination, including bacteria and fungi (Phechkrajang & Yooyong, 2017). Additionally, there is no study on the dissolution behavior and kinetics of Ca^{2+}, which passes into the solution when colemanite is dissolved in propionic acid. For this reason, investigating the dissolution kinetics of colemanite in propionic acid is important for the literature. The parameters selected for investigation in this study were the reaction temperature, solid-liquid ratio, acid concentration, stirring speed, and particle size to elucidate the dissolution of colemanite in the presence of propionic acid. The objective is to construct a kinetic model that accurately reflects the experimental outcomes.

MATERIALS AND METHODS

Material

The 66.9% purity colemanite used in the study was obtained from the boron deposits of Eti Maden İşletmeleri in the Emet-Kütahya-Türkiye area. The ore was ground in a Resch AS200 brand laboratory grinder and separated into particle size fractions of -100+150, -150+250, -250+400, and -400+600 µm diameter in ASTME-11 standards. The ore was dried in an oven at 100 °C to remove moisture content. In kinetic calculations, the arithmetic average of the lower and upper limits of the particle size given as ranges was used. The propionic acid used with 99% purity was obtained from Merck. The chemical composition of the colemanite ore employed was determined through the utilization of spectrophotometric and gravimetric methodologies, the findings of which are presented in Table 2.

Table 2. Chemical Analysis of Colemanite Ore

Component	% Composition
B_2O_3	34.21
CaO	19.24
H_2O	14.66
MgO	1.72
Moisture	0.71
Others	29.46

To determine the structural analysis of colemanite ore, the structural properties of colemanite were analyzed by scanning electron microscope (SEM) and X-ray diffraction (XRD). The SEM image is given in Figure 1, and the XRD analysis result is given in Figure 2.

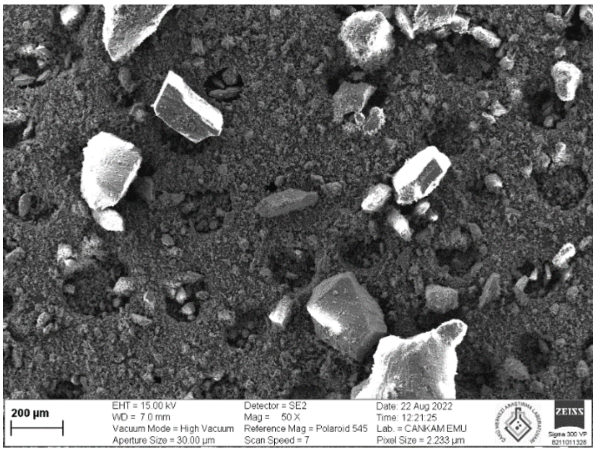

Figure 1: SEM image of colemanite ore used in the study used in the study

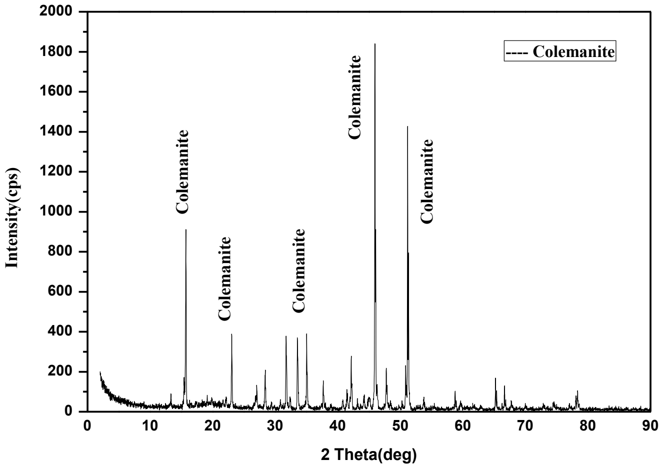

Figure 2: XRD analysis of the original colemanite ore

Method

In carrying out the experimental procedure; reaction temperature (K), solid/liquid ratio (S/L), acid concentration (C), stirring speed (W), and particle size (D) parameters were used. Table 3 presents the parameters and their corresponding levels. These parameters and their respective levels were established following a detailed analysis of the preliminary trial data and an extensive literature review.

Table 3. Parameters and Levels Selected to Examine the Kinetics of Ca^{2+} Passing İnto Solution

Parameters	**Levels**
Reaction temperature, (ºK)	283, 293, 303*,313, 323
Solid/liquid ratio, (S/L)	20, 40*, 60, 80
Acid concentration, (M)	4.05, 5.4*, 6.75, 8.1
Stirring speed, (rpm)	300, 400*,500
Gain size, (µm)	100-150,150-250, 250-400*,400-600

*Fixed levels of each parameter

Table 4. Kinetic Study Experimental Plan

Experiment No.	**Reaction temperature (K)**	**Solid/liquid ratio (S/L)**	**Acid concentration (M)**	**Mixing rate (rpm)**	**Particle size (µm)**
1	**283**	40	5.4	400	250-400
2	**293**	40	5.4	400	250-400
3	**303**	40	5.4	400	250-400
4	**313**	40	5.4	400	250-400
5	**323**	40	5.4	400	250-400
6	303	**20**	5.4	400	250-400
7	303	**60**	5.4	400	250-400
8	303	**80**	5.4	400	250-400
9	303	40	**4.05**	400	250-400
10	303	40	**6.75**	400	250-400
11	303	40	**8.1**	400	250-400
12	303	40	5.4	**300**	250-400
13	303	40	5.4	**500**	250-400
14	303	40	5.4	400	**100-150**
15	303	40	5.4	400	**150-250**
16	303	40	5.4	400	**400-600**

The dissolution kinetics of colemanite have been studied using various leach solutions, and the effects of different parameters such as reaction temperature, solid-liquid ratio, acid concentration, particle size, and stirring speed have been extensively examined.

Overall, the findings across various studies indicate that the dissolution kinetics of colemanite are significantly influenced by reaction temperature, solid-liquid ratio, acid concentration, particle size, and stirring speed. Maintaining the levels of specific parameters constant, as described in the experimental design, allows for a more precise understanding of the impact of individual parameters on the dissolution process (Table 4).

Experimental procedure

The dissolution kinetics of colemanite are influenced by several parameters, including reaction temperature, solid-to-liquid ratio, particle size, acid concentration, and stirring speed. The current experimental setup, using a double-walled glass reactor with controlled temperature and mechanical mixing (SCILOGEX brand, OS20-Pro), aligns well with the conditions studied in the literature. This setup allows for precise control and optimization (Polyscience brand and SD20R-30-A12E model) of the dissolution process, contributing to a deeper understanding of the kinetics involved (Figure 3).

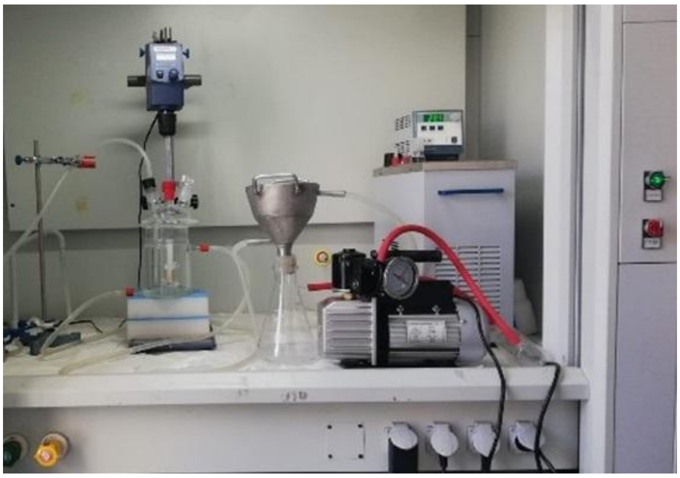

Figure 3. Experimental Setup Used in Our Experimental Study

For the dissolution process, propionic acid and distilled water were added to a certain concentration in the reactor. After the solution reached the desired equilibrium temperature, colemanite ore was added, and the dissolution process continued for the specified time. The results of each experiment were replicated on two occasions, and the mean of these replicates was employed in the calculations of kinetic analysis.

Analysis, calculations, and modeling

The multiple filtration steps at specified time intervals and the use of quantitative filter paper with a pore diameter of 2.5 micrometers are critical for accurately tracking the dissolution kinetics of colemanite. The options of filter pore size, the nature of the suspension, and the filtration conditions all play pivotal roles in ensuring efficient separation and accurate analysis of the dissolved species in the solution. These findings are supported by various studies on filtration mechanisms and dissolution kinetics in different contexts. The measurement of Ca^{2+} in the experimental solutions using AAS and expressing it as the percentage rate of passing the solution provides valuable insights into the dissolution kinetics of colemanite. The dissolution rate and Ca^{2+} transfer are influenced by various parameters, including particle size, solid/liquid ratio, propionic acid concentration, reaction temperature, and stirring speed, as demonstrated in various studies.

In summary, the kinetic modeling of the dissolution of colemanite, using percent dissolution values and the software Statistica 10, involved determining the constants (a,b,c,m), the Arrhenius constant (A), the activation energy (E), and the regression coefficient (r^2). The studies collectively highlight the significant influence of reaction conditions such as particle size, solid/liquid ratio, propionic acid concentration, reaction temperature, and stirring speed on the dissolution kinetics, demonstrating the effectiveness of simultaneous regression models in capturing these Dynamics.

RESULTS AND DISCUSSION

Reactions for Kinetic Solutions

The chemical reaction occurring in the dissolution kinetics may be expressed in the following equation:

$$4CH_3CH_2COOH_{(aq)}+4H_2O_{(\ell)}\rightarrow 4CH_3CH_2COO^{-}_{(aq)}+4H_3O^{+}_{(aq)} \quad (2)$$

When colemanite is inserted into a propionic acid solution, the reactions that occur in the environment are as follows;

$$2CaO.3B_2O_3.5H_2O_{(s)} + 2H_3O^{+}_{(aq)} \rightarrow Ca^{+2}_{(aq)} + 2H_3BO_{3\,(aq)} + CaO.2B_2O_{3(k,aq)} + 4H_2O_{(s)} \quad (3)$$

$$CaO.2B_2O_{3(k,aq)} + 2H_3O^{+}_{(aq)} \rightarrow Ca^{+2}_{(aq)} + 2H_3BO_{3\,(aq)} \quad (4)$$

$$Ca^{+2}_{(aq)} + CH_3CH_2COO^{-}_{(aq)} \rightarrow Ca(CH_3CH_2COO) \quad (5)$$

The reaction overall can be summarised as follows;

$$2CaO.3B_2O_3.5H_2O_{(s)}+4CH_3CH_2COOH_{(aq)}+2H_2O\rightarrow 2Ca^{+2}_{(aq)}+6H_3BO_{3(aq)}+4CH_3CH_2COO^{-}_{(aq)} \quad (6)$$

The XRD and SEM views of the solid residue remaining after the experiment are given in Figure 4(a) and (b), respectively. We can see the presence of Ca^{2+} derived structures such as $CaCO_3$ in colemanite in residue at the end the end of the experiment in the XRD graph in Figure 4(a). A diagram showing the dissolution process is given in Figure 5.

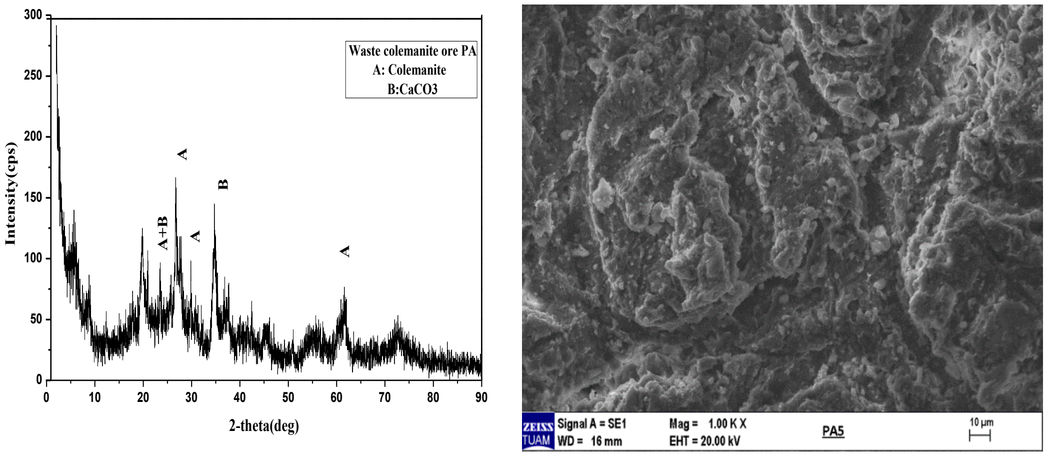

(a) (b)

Figure 4. The Solid Residue Obtained After the Experiment a) X-ray Diffractogram b) SEM Image at 1X

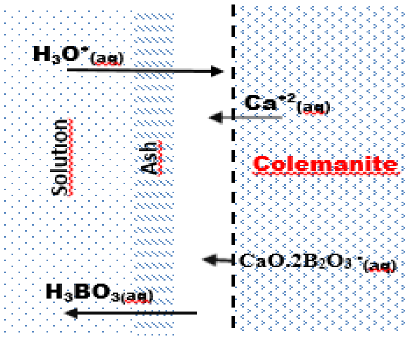

Figure 5. Schematic View of the Dissolution Process

Effect of parameters

The XRD and SEM views of the solid residue remaining after the experiment are given in Figure 4(a) and (b), respectively. We can see the presence of Ca^{2+} derived structures such as $CaCO_3$ in colemanite in residue at the end of the experiment in the XRD graph in Figure 4(a). A schematic representation of the dissolution process is presented in Figure 5.

$$\text{Dissolution fraction} X_{Ca^{2+}} = \frac{\text{Amount of } Ca^{+2} \text{ passing into solution (mg)}}{\text{The amount } Ca^{+2} \text{ in original ore (mg)}}$$

In the light of the parameters and levels specified in Table 3, graphs of the percentage of Ca^{2+} passing into the solution in the solutions obtained are drawn against time (see Figure 6-10).

Effect of temperature on leaching dissolution reaction

The studies consistently demonstrate that increasing reaction temperature enhances the rate of Ca^{2+} ions passing into solution during the dissolution of colemanite. This thermal dependence is supported by the calculated activation energies and observed dissolution rates across different leaching systems and conditions. The effect of reaction temperature on the rate of Ca^{2+} ions passing into solution was examined at temperatures of 283, 293, 303, 313, and 323°K. The graph of the obtained dissolution percentages against time is given in Figure 6. As indicated in Figure 6., the increase in temperature increased the amount of dissolution. Since the kinetic energy of molecules depends exponentially on temperature, the collision and effective collision motion of molecules will increase with increasing temperature (Bayca et al., 2014; Şimşek et al., 2018). Thus, the reaction rate increases, and as a result, the amount of Ca^{2+} passing into the solution in the aqueous environment increases.

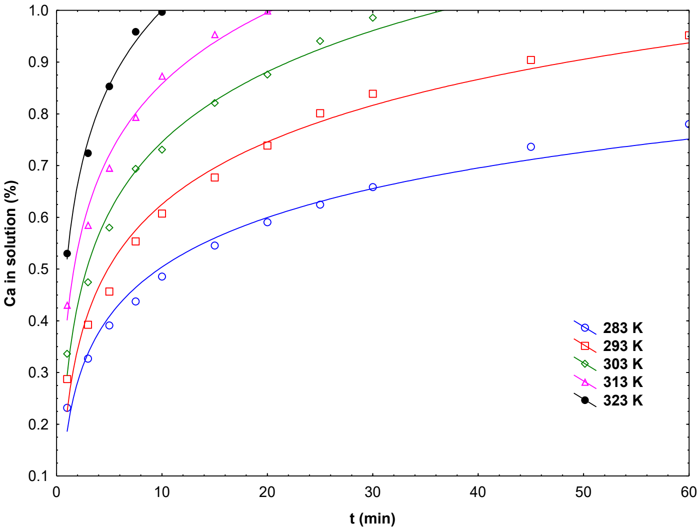

Figure 6. Effect of Reaction Temperature on Ca^{2+} Passing İnto Solution

Effect of solid-liquid ratio

The effect of the solid-liquid ratio on the rate of Ca^{2+} ions in the colemanite structure passing into the solution was examined at rates of 20, 40, 60, and 80 g/L. The dissolution curves of Ca^{2+} ions versus time are given graphically in Figure 7. As illustrated in Figure 7, the dissolution rate of Ca^{2+} is observed to increase with a decline in the solid/liquid ratio. This phenomenon can be explained by a reduction in the quantity of colemanite particles present about to the amount of propionic acid in each reagent within the reaction mixture (Abali et al., 2006; Karagöz & Kuşlu, 2017; Şimşek et al., 2018).

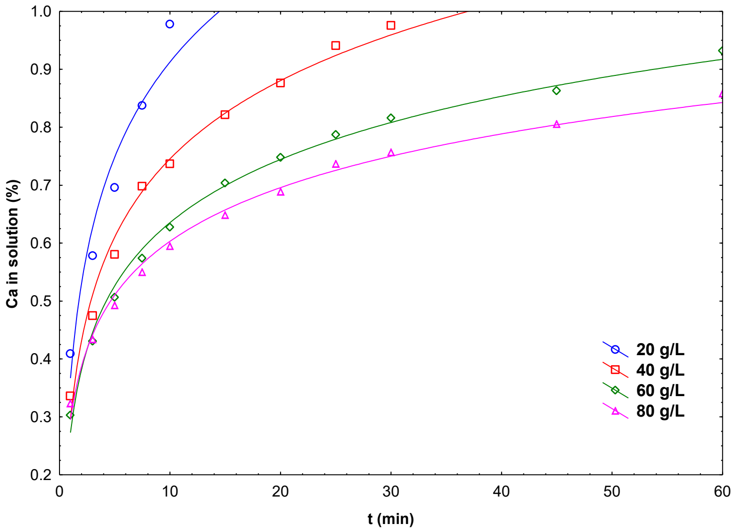

Figure 7. Effect of Solid-liquid Ratio on Ca^{2+} Passing İnto Solution

Effect of acid concentration on leaching dissolution reaction

The influence of propionic acid concentration on the rate at which Ca^{2+} ions in the colemanite structure pass into solution; 4.05, 5.4, 6.75, and 8.1 M PA were examined, and the dissolution fractions against time are given graphically in Figure 8. As illustrated in Figure 8, the dissolution rate is observed to decline with an increase in acid concentration. By dissolving propionic acid (CH_3CH_2COOH) in water, it dissociates into H_3O^+ and $CH_3CH_2COO^-$ ions, as seen in reaction 2. Since the amount of $CH_3CH_2COO^-$ per unit volume is higher at high acid concentration, $(CH_3CH_2COO)_2Ca$ formation occurs. In addition, H_3O^+ ions prevent the dissolution of the ore by forming an ash film layer around the unreacted colemanite particles (Tunc et al., 2001).

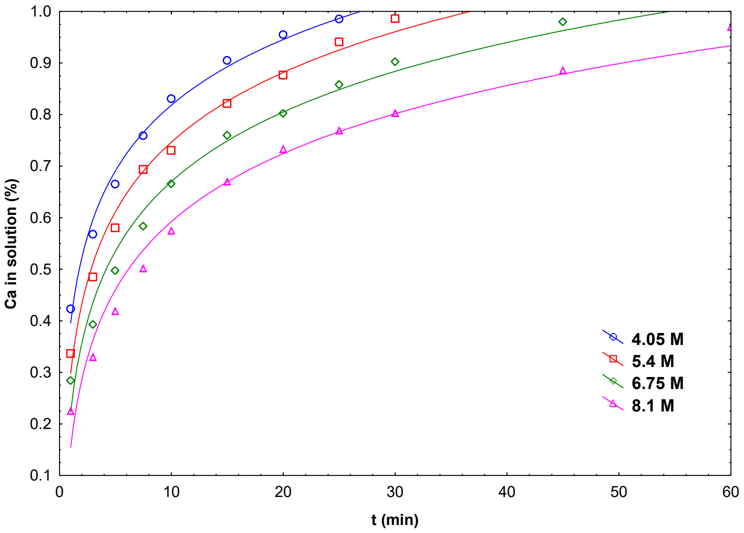

Figure 8. Effect of Propionic Acid Concentration on Ca^{2+} Passing İnto Solution

Effect of stirring speed on leaching dissolution reaction

Overall, the studies consistently show that increasing the stirring speed (300, 400 and 500 rpm) enhances the dissolution rate of Ca^{2+} ions from colemanite. Higher stirring speeds improve the mass transfer between the solid and liquid phases by promoting better mixing and reducing the thickness of the boundary layer. This leads to more efficient dissolution kinetics across different experimental conditions and leaching systems. Dissolution fractions against time are given graphically in Figure 9. Homogeneous mixing of the solution occurs at 400 rpm stirring. As seen in Figure 9., it shows that the stirring speed has a negligible difference in the rate of Ca^{2+} ions passing into the solution. For this reason, this data was not used in the kinetic model equation. Ozmetin et al. acetic acid (Özmetin et al., 1996), Alkan et al. oxalic acid (Alkan & Doğan, 2004), Kızılca et al. found similar results for the dissolution kinetics of colemanite (Kizilca & Copur, 2015) in methanol-saturated water.

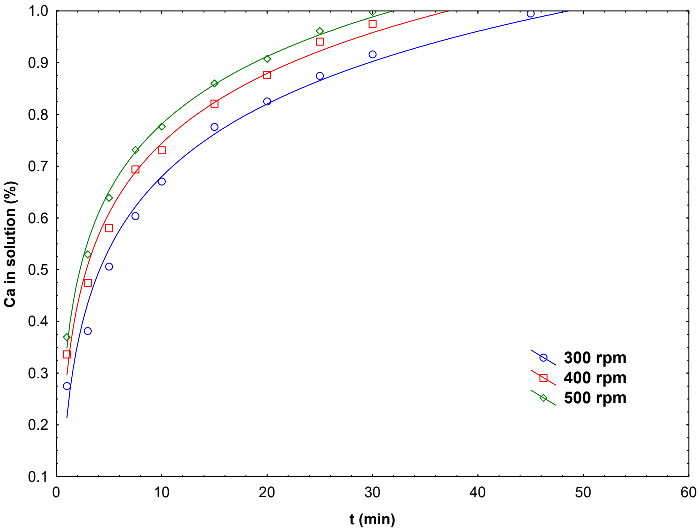

Figure 9. Effect of Stirring Speed on Ca^{2+} Passing to Solution

Effect of particle size on the leaching dissolution reaction

The studies consistently demonstrate that decreasing particle size (100-150, 150-250, 250-400, and 400-600 µm) enhances the dissolution rate of Ca^{2+} ions from colemanite. The increased surface area available for reaction at smaller particle sizes significantly improves the mass transfer and dissolution efficiency, as evidenced by the various experimental and kinetic models.

Experiments were carried out on the rate of Ca^{2+} ions in colemanite passing into solution using particle size ranges of 100-150, 150-250, 250-400, and 400-600 µm. The graph of the transition values of Ca^{2+} ions into solution aganist time is given in Figure 10. As illustrated in Figure 10., decreasing the particle size increases the rate at which Ca^{2+} ions pass into the solution. It is observed that the amount of Ca^{2+} passing into the solution increases as the surface area of the solid amount per amount of solvent increases as the particle size decreases.This highlights the importance of particle size in influencing the dissolution kinetics (Uğur, 2024b).

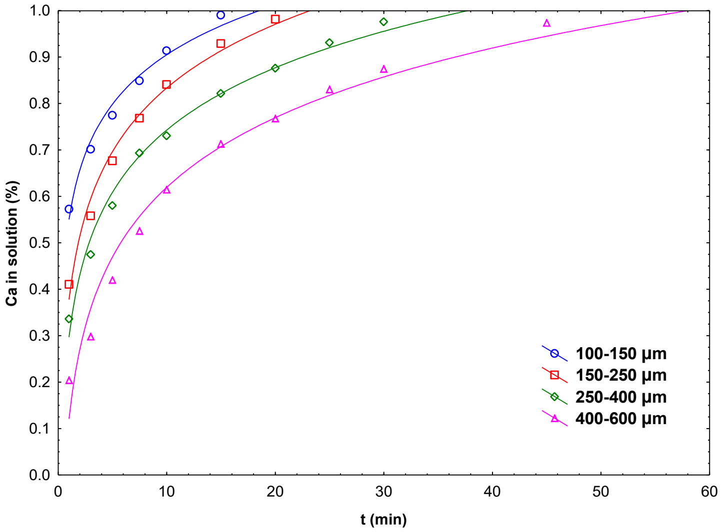

Figure 10. Effect of Reaction Particle Sizes on Ca^{2+} Passing İnto Solution

Kinetic analysis of leaching dissolution reaction

In summary, the studies collectively demonstrate the significant influence of reaction conditions such as particle size, solid-liquid ratio, acid concentration, reaction temperature, and stirring speed on the dissolution kinetics of colemanite. These findings highlight the effectiveness of chemical kinetics in optimizing industrial processes for boric acid production (Uğur, 2024b). In summary, both homogeneous and heterogeneous reaction models have been applied to understand the kinetics of Ca^{2+} transfer in the dissolution of colemanite. The choice of model depends on the specific conditions and mechanisms influencing the dissolution process. For surface-controlled reactions, homogeneous models like the Avrami model provide valuable insights, while for diffusion-controlled processes, heterogeneous models such as the particle-grain model are more appropriate. The activation energy and other kinetic parameters derived from these studies are crucial for optimizing industrial processes involving colemanite dissolution (Demirkıran, 2009).

Determination of kinetic model

This study examined the kinetics of Ca^{2+} passing into the solution during the dissolution of colemanite in a propionic acid solution. This analysis employed two models: the first, a homogeneous reaction model, and the second, a heterogeneous reaction model. The suitability of the process for heterogeneous reaction models is seen from the r^2 (regression) values in Table 5. If the effect of dissolution rate on temperature is very sensitive, the reaction rate can be considered to be controlled by the chemical reaction, otherwise it can be considered to fit the diffusion-controlled model (Mazet, 1992). As seen in Figure 6, temperature change does not affect the dissolution sensitively and increases the accuracy of the model. It is concluded that the ineffective stirring speed does not contribute to the dissolution rate, which affects the dissolution process (Demir et al., 2020). In determining the rate control model of the process, the reaction rate equations were tested one by one according to the control steps, using the percentage values of Ca^{2+} passing into a solution for all factors and levels. r^2 (regression) values are calculated and given in Table 5.

Table 5. Homogeneous and Heterogeneous Reaction Rate Equations and Regression (r^2) Values Tried in Modeling

Equations	**Type of rate control**	**r^2**
$kt = 1 - 3(1-X)^{2/3} + 2(1-X)$	Ash film diffusion control for fixed-size spheres	**0.9768**
$kt = 1 - (1-X)^{1/3}$	Chemical reaction control	0.8431
$kt = 1 - (1-X)^{1/2}$	Fluid film diffusion control for shrinking spheres (large grain)	0.6765
$kt = 1 - (1-X)^{2/3}$	Fluid film diffusion control shrinking spheres (small grain)	0.2989
$kt = -\ln(1-X)$	First order pseudo homogenous reaction model	0.9084
$kt = X/(1-X)$	Second order pseudo homogenous reaction model	0.2666
$kt^m = -\ln(1-X)$	Avrami model	0.9089
$kt = X^2$	Ash film diffusion control for fixed-size flat plate	0.8463

The highest regression (r^2) value given in Table 5 shows that the speed expression of the process fits the "ash film diffusion control for fixed-size spherical particles" model. To determine the suitability of this model the impact of each parameter on the model equation was evaluated. The integrated rate expression for the ash film diffusion control model is given in equation 7:

$$kt = 1 - 3(1-X)^{2/3} + 2(1-X) \quad (7)$$

Since there is a linear relationship between $1-3(1-X)^{2/3}+2(1-X)$ and time (t), $1-3(1-X)^{2/3}+2(1-X)$ versus t for each parameter graph must be linear. Figures 11-14 show the reaction temperature, solid/liquid ratio, propionic acid concentration, and particle size graphs, presented in a graphical format. These linear graphs show that the reaction rate expression is controlled by the diffusion model from the ash (product) film.

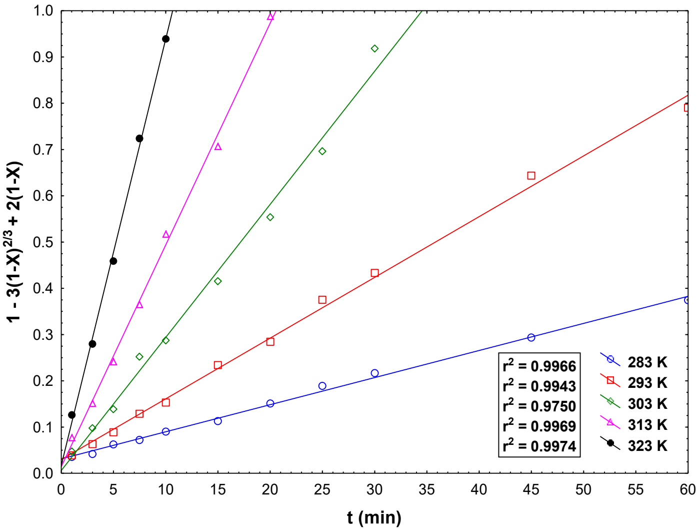

Figure 11. Variation of 1- 3(1-X)$^{2/3}$ + 2(1-X) with Respect to t for Different Temperatures of the Leaching Dissolution Reaction

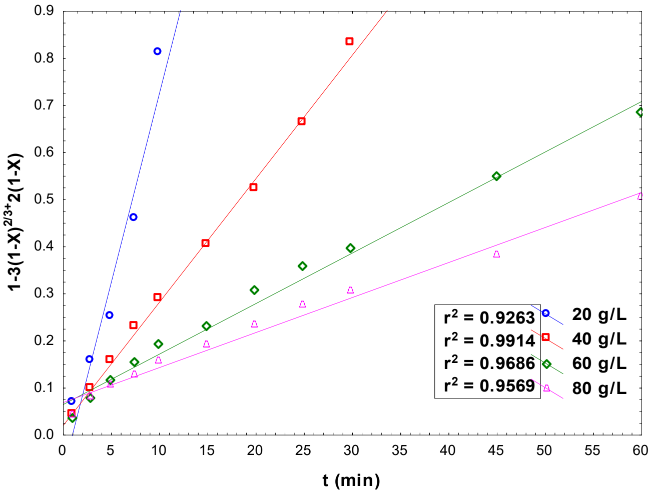

Figure 12. Variation of 1- 3(1-X)$^{2/3}$ + 2(1-X) with Respect to t for Different Solid-liquid Ratio of the Leaching Dissolution Reaction

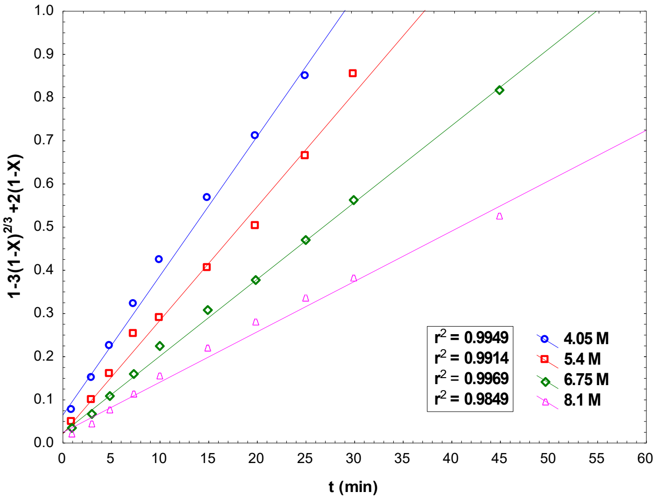

Figure 13. Variation of 1- 3(1-X)$^{2/3}$ + 2(1-X) with Respect to t for Different Propionic Acid Concentrations of the Leaching Dissolution Reaction

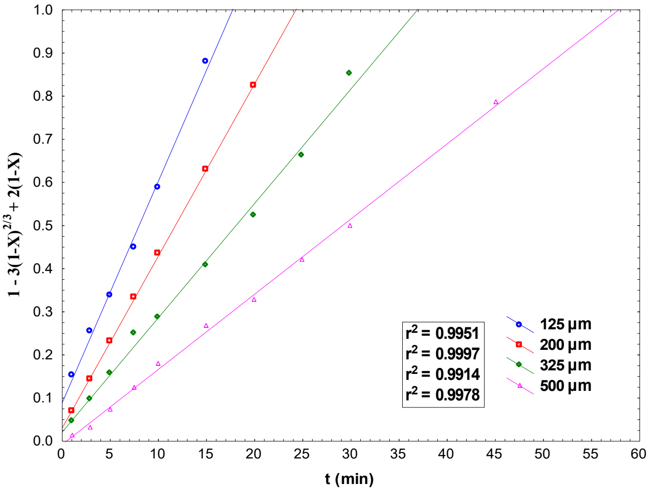

Figure 14. Variation of 1- $3(1\text{-}X)^{2/3}$ + 2(1-X) with Respect to t for Different Particle Size of the Leaching Dissolution Reaction

Leaching dissolution reaction calculation of activation energy and arrhenius constant

The Arrhenius equation effectively describes the relationship between the reaction rate constant (k) and temperature (T) for the dissolution of colemanite in various acidic solutions. The exponential behavior of (k) concerning (T) is consistent across different studies, with activation energies ranging from 21.08 kj/mol to 59.03 kj/mol, highlighting the robustness of the Arrhenius equation in chemical kinetics (Abanades et al., 2015; Naktiyok et al., 2013).

$$k=Ae^{-E/RT} \tag{8}$$

Equation 9 is obtained by performing a natural logarithmic transformation of the Arrhenius equation given in Equation 8.

$$\ln k = \ln A - \frac{E}{RT} \tag{9}$$

The activation energy is defined by calculating the slope of a graph representing the values of -lnk versus temperature, expressed in kelvins (Kuşlu et al., 2010). Figure 15 shows the Arrhenius graph.

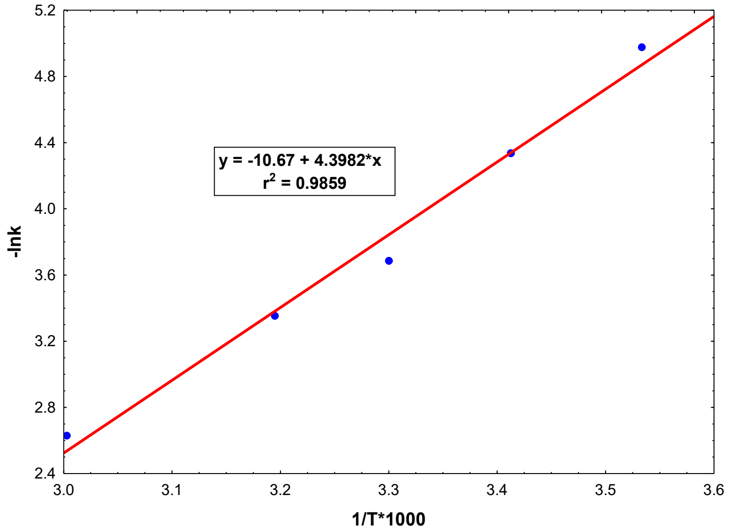

Figure 15. The Lnk is Against 1/T(K)*1000

Activation energy and Arrhenius constants were determined from the slope of the Arrhenius graph in Figure 15. The activation energy was calculated as 36.56 kj/mol and the Arrhenius constant (A) as $5.19*10^6$. The activation energy of the process is less than 40 kj/mol, which corroborates the hypothesis that the dissolution rate is governed by the diffusion model from the ash (product) film (Uğur, 2024b). The relationship between the rate constant (k) in the diffusion model from the ash film in Equation 7 and the solid/liquid ratio, propionic acid concentration, and particle size is given in Equation 10.

$$k=A.\ (KS)^{a}\ .(C)^{b}.\ (D)^{c}\ .e^{-E/RT} \qquad (10)$$

Equation 10 is written instead of the rate constant k in the diffusion model from the ash film in Equation 7 and Equation 11 is obtained.

$$1 - 3(1-X_{Ca^{+2}})^{2/3} + 2(1-X_{Ca^{+2}}) = A.\ (KS)^{a}.\ (C)^{b}.\ (D)^{c}.\ e^{-E/RT} *t \qquad (11)$$

The values of the exponential constants a, b, and c were obtained via a statistical calculation utilizing multiple regression analysis with the Statistica 10 software package. The exponential constants were calculated as -1.53, -1.42, and -0.948, respectively. These constants were written in Equation 11. and a semi-empirical mathematical expression of the diffusion model from the ash film was obtained depending on the parameters as in Equation 12.

$$1\text{-}3(1-X_{Ca^{+2}})^{2/3} + 2(1-X_{Ca^{+2}}) = 5.19*10^{6}\ (KS)^{-1.53}.\ (C)^{-1.42}.(D)^{-0.948}.\ e^{\frac{-36.56}{R*T}} *t \qquad (12)$$

Validation of the kinetic model

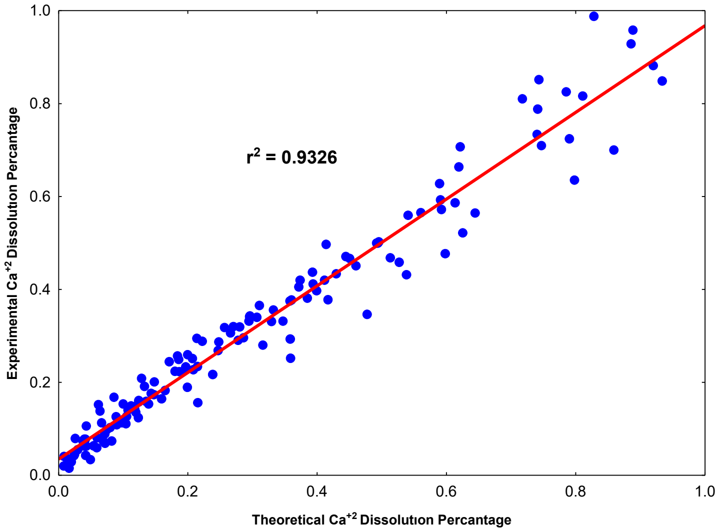

Figure 16. Compatibility of Experimental and Theoretical Transformation Data

Theoretical dissolution values ($X_{theoretical}$) were determined with the help of the semi-empirical mathematical equation in equation 12, and experimental dissolution values ($X_{experimental}$) were defined as trial results. To determine the compatibility of the model with experimental data, Xtheoretical versus Xexperimental data are plotted in Figure 16. The observation that the theoretical and experimental dissolution data are aligned along a single diagonal on the graph indicates a concordance between the determined model and the experimental outcomes.

CONCLUSION

In this study, the kinetics of Ca^{2+} transfer to the solution in the dissolution of colemanite in propionic acid solution was examined. Obtained results;

- ✓ As the reaction temperature increases, the amount and transition rate of Ca^{2+} passing into the solution increases.

- ✓ As the solid-liquid ratio, acid concentration, and particle size increase, the rate of Ca^{2+} passing into the solution decreases. The results demonstrate that the stirring speed has no notable impact on the dissolution process.
- ✓ We determined that propionic acid, which has weak acidic properties, can dissolve colemanite ore for the production of boric acid. It is considered to be a new solvent reactant for the production of boric acid and does not form an environmentally harmful by-product (borogypsum). Additionally, calcium propionate ($Ca(CH_3CH_2COO)$, which is environmentally friendly, has commercial value, and is used in the food industry, is formed as a by-product.
- ✓ In conclusion, the experimental data analyzed using both homogeneous and heterogeneous models consistently indicate that the dissolution of Ca^{2+} ions from colemanite in an aqueous environment fits the "diffusion controlled from product (ash) film" model. The calculated activation energy of 36.56 kj/mol aligns well with values reported in other studies, further validating this dissolution kinetics model.
- ✓ A semi-empirical mathematical model was constructed based on a series of specified parameters;

$$1\text{-}3(1\text{-}X_{Ca^{+2}})^{2/3} + 2(1\text{-}X_{Ca^{+2}}) = 5.19*10^{6}\ (S/L)^{-1.53}.\ (C)^{-1.42}.(D)^{-0.948}.\ e\frac{-36.56}{R*T}\ *t$$

ACKNOWLEDGEMENTS

This research was carried out with the support of the Scientific Research Project (MF210621D06) funded by Çankırı Karatekin University. Authors thank to Çankırı Karatekin University, Scientific Research Project Management Unit (ÇAKÜ-BAP).

Conflict of Interest

The article authors declare that there is no conflict of interest between them.

Author's Contributions

The authors declare that they have contributed equally to the article.

REFERENCES

Abali, Y., Bayca, S., & Mistincik, E. (2006). Kinetics of oxalic acid leaching of tincal. *Chemical Engineering Journal*, *123*(1-2), 25-30.

Abanades, S., Kimura, H., & Otsuka, H. (2015). Kinetic investigation of carbon-catalyzed methane decomposition in a thermogravimetric solar reactor. *International Journal of Hydrogen Energy*, *40*(34), 10744-10755.

Alkan, M., Çifçi, C., Ayaz, F., & Doğan, M. (2000). Dissolution kinetics of ulexite in aqueous EDTA solutions. *Canadian Metallurgical Quarterly*, *39*(4), 433-440.

Alkan, M., & Doğan, M. (2004). Dissolution kinetics of colemanite in oxalic acid solutions. *Chemical Engineering and Processing: Process Intensification*, *43*(7), 867-872.

Bayca, S. U., Kocan, F., & Abali, Y. (2014). Dissolution of colemanite process waste in oxalic acid solutions. *Environmental Progress & Sustainable Energy*, *33*(4), 1111-1116.

Çalımlı, M. H., Mehmet, T., & Kocakerim, M. M. (2020). Investigation dissolution behaviours and kinetics parameters of ulexite in boric acid solution. *International Journal of Chemistry and Technology*, *4*(2), 121-129.

Çavuş, F., & Kuşlu, S. (2005). Dissolution kinetics of colemanite in citric acid solutions assisted by mechanical agitation and microwaves. *Industrial & Engineering Chemistry Research*, *44*(22), 8164-8170.

Çopur, M., Pekdemir, T., Kocakerim, M. M., Korucu, H., & Guliyev, R. (2022). Industrial symbiosis: Boron waste valorization through CO2 utilization. *Korean Journal of Chemical Engineering*, *39*(10), 2600-2614.

Demir, F., Al-Ani, A. O. A., & Lacin, O. (2020). A kinetic analysis for production of calcium borogluconate from colemanite. *International Journal of Chemical Kinetics*, *52*(11), 769-776.

Demirkıran, N. (2009). Dissolution kinetics of ulexite in ammonium nitrate solutions. *Hydrometallurgy*, *95*(3-4), 198-202.

Guliyev, R., Kuşlu, S., Çalban, T., & Çolak, S. (2012). Leaching kinetics of colemanite in ammonium hydrogen sulphate solutions. *Journal of Industrial and Engineering Chemistry*, *18*(4), 1202-1207.

Gür, A. (2007). Dissolution mechanism of colemanite in sulphuric acid solutions. *Korean Journal of Chemical Engineering*, *24*(4), 588-591.

Gür, A., & Alkan, M. E. (2008). Leaching kinetics of colemanite in perchloric acid solutions. *journal of chemical engineering of japan*, *41*(5), 354-360.

Karagöz, Ö., & Kuşlu, S. (2017). Dissolution kinetics of colemanite in potassium dihydrogen phosphate solution (KH2PO4). *International Journal of Hydrogen Energy*, *42*(36), 23250-23259.

Kavcı, E., Calban, T., Colak, S., & Kuşlu, S. (2014). Leaching kinetics of ulexite in sodium hydrogen sulphate solutions. *Journal of Industrial and Engineering Chemistry*, *20*(5), 2625-2631.

Kaya, F., & Özer, A. (2024). Production of boric acid from colemanite ore in the semi-batch reactor: Investigation of product yield and impurity control. *Minerals Engineering*, *206*, 108528.

Kizilca, M., & Copur, M. (2015). Kinetic investigation of reaction between colemanite ore and methanol. *Chemical Engineering Communications*, *202*(11), 1528-1534.

Kum, C., Alkan, M., & Kocakerim, M. M. (1994). Dissolution kinetics of calcined colemanite in ammonium chloride solution. *Hydrometallurgy*, *36*(2), 259-268.

Kurtbaş, A., Kocakerim, M. M., Küçük, Ö., & Yartaşı, A. (2006). Dissolution of colemanite in aqueous solutions saturated with both sulfur dioxide (SO2) gas and boric acid. *Industrial & engineering chemistry research*, *45*(6), 1857-1862.

Kuşlu, S., Dişli, F. Ç., & Çolak, S. (2010). Leaching kinetics of ulexite in borax pentahydrate solutions saturated with carbon dioxide. *Journal of Industrial and Engineering Chemistry*, *16*(5), 673-678.

Küçük, N., Küçük, Ö., & Solak, A. O. (2023). Optimization by Using the Taguchi Method of Boric Acid Production by Dissolving Flash Calcined Colemanite in Water Saturated with SO2. *Iran. J. Chem. Chem. Eng. Research Article Vol*, *42*(5).

Küçük, Ö., Kocakerim, M. M., Yartaşı, A., & Çopur, M. (2002). Dissolution of kestelek's colemanite containing clay minerals in water saturated with sulfur dioxide. *Industrial & engineering chemistry research*, *41*(12), 2853-2857.

Künkül, A., Aslan, N. E., Ekmekyapar, A., & Demirkıran, N. (2012). Boric acid extraction from calcined colemanite with ammonium carbonate solutions. *Industrial & engineering chemistry research*, *51*(9), 3612-3618.

Mazet, N. (1992). Modeling of gas-solid reactions. 2. nonporous solids. *Int. Chem. Eng.*, *32*, 271-284.

Naktiyok, J., Bayrakçeken, H., Özer, A. K., & Gülaboğlu, M. Ş. (2013). Kinetics of thermal decomposition of phospholipids obtained from phosphate rock. *Fuel processing technology*, *116*, 158-164.

Özmetin, C., Kocakerim, M. M., Yapıcı, S., & Yartaşı, A. (1996). A semiempirical kinetic model for dissolution of colemanite in aqueous CH3COOH solutions. *Industrial & engineering chemistry research*, *35*(7), 2355-2359.

Phechkrajang, C. M., & Yooyong, S. (2017). Fast and simple method for semiquantitative determination of calcium propionate in bread samples. *journal of food and drug analysis*, *25*(2), 254-259.

Sert, H., Yıldıran, H., & Toscalı, D. (2012). An investigation on the production of sodium metaborate dihydrate from ulexite by using trona and lime. *International journal of hydrogen energy*, *37*(7), 5833-5839.

Şimşek, H. M., Guliyev, R., & Beşe, A. V. (2018). Dissolution kinetics of borogypsum in di-ammonium hydrogen phosphate solutions. *international journal of hydrogen energy*, *43*(44), 20262-20270.

Şimşek, H. M., & Yeşilyurt, M. (2021). Sodyumbisülfat çözeltisinde kolemanitin kinetik mekanizmasının araştırılması. *BOR DERGİSİ*, *6*(4), 395-401.

Temur, H., Yartaşı, A., Copur, M., & Kocakerim, M. M. (2000). The kinetics of dissolution of colemanite in H3PO4 solutions. *Industrial & engineering chemistry research*, *39*(11), 4114-4119.

Tombal, T., Özkan, Ş., Kurşun Ünver, İ., & Osmanlioğlu, A. (2016). Properties, production, uses of boron compounds and their importance in nuclear reactor technology. *Boron*, *1*(2), 86-95.

Tunc, M., Yapici, S., Kocakerim, M., & Yartasi, A. (2001). The dissolution kinetics of ulexite in sulphuric acid solutions. *equilibrium*, *3*, 2.

Tunç, M., Kocakerim, M. M., Küçük, Ö., & Aluz, M. (2007). Dissolution of colemanite in (NH 4) 2SO 4 solutions. *Korean Journal of Chemical Engineering*, *24*(1), 55-59.

Uğur, M. (2024a). Dissolution behavior and kinetic investigation of [Ca]^(2+) in the dissolution of colemanite in propionic acid presence saturated with synthetic flue gas. *Journal of Boron*, *9*(1), 9-18.

Uğur, M. (2024b). Dissolution Kinetics for Colemanite Ore in Propionic Acid Solutions Saturated with Pyrite Roasting Gas. *Iranian Journal of Chemistry and Chemical Engineering*(Articles in Press).

Uğur, M. (2024c). Dissolution behavior and kinetic investigation of in solution in the reaction of colemanite ore with propionic acid. *International Journal of Chemistry and Technology*, *8*(2), 143-152.